ELSEVIER

Journal of Organometallic Chemistry 659 (2002) 22–28

Journal of Organo metallic Chemistry

www.elsevier.com/locate/jorganchem

Synthesis, reactivity and structures of ruthenium carbonyl clusters with telluride and hydride ligands

Martin Brandl [a], Henri Brunner [a], Helene Cattey [b], Yves Mugnier [b], Joachim Wachter [a,*], Manfred Zabel [a]

[a] *Institut für Anorganische Chemie der Universität Regensburg, D-93040 Regensburg, Germany*

[b] *Laboratoire de Synthèse et d'Electrosynthèse Organométalliques (UMR 5632), Université de Bourgogne, F-21100 Dijon, France*

Received 4 April 2002; accepted 3 June 2002

Abstract

The reaction of $[Cp^*_2Nb(Te_2H)]$ (**1**) ($Cp^* = C_5Me_5$) with $[Ru_3(CO)_{12}]$ in boiling toluene gave $[Ru_3(\mu_2\text{-}H)_2(CO)_9(\mu_3\text{-}Te)]$ (**2**), $[Ru_6(\mu_3\text{-}H)(CO)_{15}(\mu_3\text{-}Te)_3][Cp^*_2Nb(CO)_2]$ (**3**) and $[Ru_5(\mu_2\text{-}H)(CO)_{14}(\mu_4\text{-}Te)][Cp^*_2Nb(CO)_2]$ (**4**) along with already known $[Ru_4(CO)_{11}(\mu_4\text{-}Te)_2]$ (**5**). Complexes **2**–**4** were analytically and spectroscopically characterized and X-ray diffraction analyses of **3** and **4** were carried out. The anion of **3** is built up of a triangular hexametallic core of C_{3v} symmetry, in which the central Ru_3 triangle, being bridged by a μ_3-H ligand, is composed of three corner-linked Ru_3Te tetrahedra. The main structural feature of the anion of **4** is a Ru_5Te octahedron. The cations in **3** and **4** are known niobocenedicarbonyl species. The reaction of **2** with bis(diphenylphosphino)methane (dppm) gave $[Ru_3(\mu_2\text{-}H)_2(CO)_7(dppm)(\mu_3\text{-}Te)]$ (**6**). Low temperature ^{1}H-NMR spectroscopy and X-ray diffraction analysis show an unsymmetrical distribution of both hydride ligands over the triangular Ru_3 basis of the Ru_3Te tetrahedron. The reaction of **5** with dppm gave $[Ru_3(CO)_7(dppm)(\mu_3\text{-}Te)_2]$ (**7**) and known $[Ru_4(CO)_9(dppm)(\mu_4\text{-}Te)_2]$ (**8**). The crystal structure of **7** reveals a square pyramidal arrangement of the Ru_3Te_2 core. Electrochemical studies of **5** show this complex to be able to consume up to four electrons in reversible steps. © 2002 Elsevier Science B.V. All rights reserved.

Keywords: Ruthenium; Tellurium; Carbonyl ligands; Cluster chemistry

1. Introduction

The actual interest in the chemistry of ruthenium chalcogenido clusters is mainly focussed on the combination of sulfido [1] and selenido [2] ligands with $Ru(CO)_n$ ($n = 2$, 3, 4) fragments and the investigation of the reactivity potential of the resulting products. By contrast only a few examples of ruthenium clusters with bridging tellurium ligands have been structurally characterized thus far [3,4]. This may be explained by the apparent lack of suitable Te transfer reagents, although there are numerous synthetic routes towards metal telluride clusters starting from other binary transition metal carbonyls [5].

Recently, we described the synthesis of $[Cp^*_2Nb(\eta^2\text{-}Te_2H)]$ [6] (**1**) ($Cp^* = \eta\text{-}C_5Me_5$) and its application in the synthesis of transition-metal telluride clusters [7]. Its reactions with binary metal carbonyls are characterized by the deliberation of 'active' Te ligands from the unique η^2-Te_2H ligand and the ability of the niobocene fragment to serve as redox-active CO ligand acceptor, leading to a series of novel structures. Here, we report on the reaction of **1** with $[Ru_3(CO)_{12}]$ as a new synthetic route for the formation of neutral or salt-like ruthenium clusters with three, four, five and six metal atoms, held together by μ_3- or μ_4-Te bridges, and in some cases μ_2- or μ_3-hydrido ligands.

* Corresponding author. Tel.: +49-941-943-4419; fax: +49-941-943-44139

E-mail address: joachim.wachter@chemie.uni-regensburg.de (J. Wachter).

PII: S0022-328X(02)01663-7

2. Results

2.1. The reaction of [$Ru_3(CO)_{12}$] with [$Cp^*_2Nb(Te_2H)$] (1)

The reaction of **1** with two equivalents of [$Ru_3(CO)_{12}$] in boiling toluene gave after chromatographic work-up yellow **2** (11% yield), orange **3** (4%), red–brown **4** (31%) and orange–brown **5** (27%) (Scheme 1). All compounds were investigated by means of IR, ^{1}H-NMR and mass spectra as well as elemental analyses. X-ray diffraction studies were carried out on complexes **3**–**5**. The result of the structure determination of **5** was completely identical with that of octahedral [$Ru_4(CO)_{11}(\mu_4\text{-Te})_2$], which had been obtained from [$Ru_3(CO)_{12}$] and [$Fe_3(CO)_9Te_2$] in poor yield [3].

Complex **2** has been identified as [$Ru_3(\mu_2\text{-H})_2(CO)_9(\mu_3\text{-Te})$], spectroscopic data of which are identical with those of a product obtained in low yields from [$Ru_3(CO)_{12}$] and TeO_3 [8] or from [$Ru_3(CO)_{12}$] and elemental tellurium (35 bar of CO/H_2) [9]. However, complete characterization was not achieved in these reports. Since then the related 48 valence electron clusters [$M_3H_2(CO)_9Te$] (M = Fe [10]; M = Os [11]) were prepared while a crystal structure determination was carried out on [$Os_3H_2(CO)_9Te$] [11]. As **2** did not crystallize well we investigated its reaction with bis(diphenylphosphino)methane (dppm), which gave the orange complex **6** (see below).

The IR spectrum of **3** contains four strong absorptions typical of terminal CO bands. The ^{1}H-NMR spectrum exhibits two singlets at $\delta = -36.45$ and $\delta = 1.94$ in a ratio 1:30, which may be assigned to μ_3-H and C_5Me_5 hydrogens, respectively. This finding is consistent with the presence of a [$Cp^*_2Nb(CO)_2$]$^+$ cation and a [$Ru_6H(CO)_{15}Te_3$]$^-$ anion. Positive and negative ESI mass spectra exhibit each ion respectively. The negative mass spectrum indicates in addition successive loss of eight CO groups.

The composition of **3** is confirmed by an X-ray crystallographic investigation. The molecular structure of the anion consists of a Ru_3 triangle composed of three corner-linked Ru_3Te tetrahedra (Fig. 1). Their Te vertices are co-oriented at one side whereas the wingtips of their Ru_3 bases form a shallow bowl. In the centre of this bowl and bridging the central Ru_3 triangle a μ_3-H ligand has been found in the difference Fourier map. Due to the EAN rule **3** has 92 valence electrons. There are two kinds of Ru–Ru bonds (Table 1). Those

$$[Ru_3(CO)_{12}] + [Cp^*{}_2NbTe_2H]\ (\mathbf{1}) \xrightarrow[115\ ^\circ C]{toluene} [Ru_3H_2(CO)_9Te]\ (\mathbf{2}) + [Cp^*{}_2Nb(CO)_2][Ru_6H(CO)_{15}Te_3]\ (\mathbf{3}) + [Cp^*{}_2Nb(CO)_2][Ru_5H(CO)_{14}Te]\ (\mathbf{4}) + [Ru_4(CO)_{11}Te_2]\ (\mathbf{5})$$

Scheme 1.

forming the central triangle are by ca. 0.2 Å longer than those forming the peripheral Ru–Ru bonds. Planar triangular hexametallic metal clusters with C_{3v} symmetry are rare, and as far as we know the only known example is the sulfur analogue of **3** [12]. A comparison of both cluster cores reveals an elongation of all ‘inner’ and ‘outer’ Ru–Ru bonds by 0.04–0.1 Å in **3** due to the larger size of Te. The structure of the [$Cp^*_2Nb(CO)_2$]$^+$ cation is identical with those observed in [$Co_{11}(CO)_{10}Te_7$][$Cp^*_2Nb(CO)_2$] [7] or [$Fe_3H(CO)_9Te$]-[$Cp^*_2Nb(CO)_2$] [13] cluster salts.

The IR spectrum of **4** reveals three strong absorptions in the range of terminal CO ligands and one absorption in the CO bridging region. The ^{1}H-NMR spectrum shows resonances at $\delta = -12.2$ and 1.94 in a ratio 1:30, they are assigned to μ_2-H and C_5Me_5 hydrogens. ESI mass spectra of **4** exhibit peaks attribuable to a [$Cp^*_2Nb(CO)_2$]$^+$ cation and a [$Ru_5H(CO)_{14}Te$]$^-$ anion, respectively. The negative mass spectrum shows four peaks characteristic of successive loss of CO groups.

An X-ray crystallographic study of **4** reveals a slightly distorted square-pyramidal Ru_5 geometry spanned by a μ_4-Te ligand (Fig. 2). Three edges of the nearly square basis are bridged in a slightly unsymmetric manner by CO ligands. The fourth edge may be spanned by a hydrogen bridge, for this bond [$d\{$Ru(1)–Ru(4)$\}$ = (3.025(1) Å] is significantly longer than the other ones [d_{mean} = 2.830(1) Å] of the Ru_4 square (Table 1). The presence of a hydride ligand is in agreement with the ^{1}H-NMR spectrum and it is also supported by the fact that hydrogen bridges tend to lengthen the concerned metal–metal bond [14]. All Ru–Ru and Ru–Te distances are comparable to those in [$Ru_4(CO)_{11}(\mu_4\text{-Te})_2$] (**5**) [3]. The cluster anion of **4** has 74 valence electrons. According to the Wade–Mingos rules it is a *closo*-octahedron with seven sceletal electron pairs. Thus, it may be derived from the class of neutral clusters of the type [$Ru_5(CO)_{15}X$] (X = S, Se, Te), for which as the only actual representative [$Ru_5(CO)_{15}S$] has been synthesized thus far [15]. As in the structure for **3** there are no peculiarities for the [$Cp^*_2Nb(CO)_2$]$^+$ cation [7,13].

2.2. The reaction of 2 and 5 with dppm

The reaction of **2** with one equivalent of dppm gave the orange complex [$Ru_3(\mu_2\text{-H})_2(CO)_7(dppm)(\mu_3\text{-Te})$] (**6**). Its composition was confirmed by means of field desorption (FD) mass spectrum and elemental analyses. The IR spectrum exhibits five strong bands typical of terminal CO groups. The ^{1}H-NMR spectrum at room temperature consists of three groups of signals: A singlet at $\delta = -17.95$ for RuH, a multiplet at $\delta = 3.67$ for CH_2 and a multiplet at $\delta = 7.27-7.48$ for the C_6H_5 rings. Monitoring the RuH resonance at low temperatures reveals a dynamic process ($k = 687\ s^{-1}$, $\Delta G^{\ddagger}_{249} = 11.45 \pm 0.5$ kcal mol^{-1}) which is frozen at -90 °C. The low

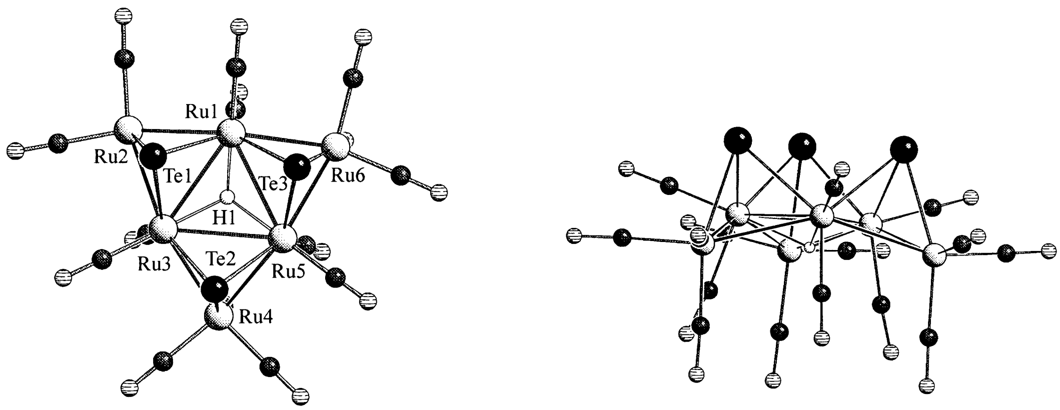

Fig. 1. Molecular structure of the $[Ru_6H(CO)_{15}Te_3]^-$ anion of **3** in top (left) and side (right) views.

Table 1
Selected bond lengths (Å) and angles (°) for $[Ru_6H(CO)_{15}Te_3][Cp^*2Nb(CO)_2]$ (**3**), $[Ru_5H(CO)_{14}Te][Cp^*2Nb(CO)_2]$ (**4**), $[Ru_3(CO)_7H_2(dppm)Te]$ (**6**) and $[Ru_3(CO)_7(dppm)Te_2]$ (**7**)

	3	**4**	**6**	**7**
Bond lengths				
Ru(1)–Ru(2)	2.820(1)	2.826(1)	2.970(1)	2.871(1)
Ru(1)–Ru(3)	3.099(1)		2.913(1)	
Ru(1)–Ru(4)		3.025(1)		
Ru(1)–Ru(5)	3.086(1)	2.931(1)		
Ru(1)–Ru(6)	2.819(1)			
Ru(2)–Ru(3)	2.821(1)	2.847(1)	2.790(1)	2.945(1)
Ru(2)–Ru(5)		2.843(1)		
Ru(3)–Ru(4)	2.830(1)	2.818(1)		
Ru(3)–Ru(5)	3.146(1)	2.861(1)		
Ru(4)–Ru(5)	2.827(1)	2.923(1)		
Ru(5)–Ru(6)	2.818(1)			
Ru(1)–Te(1)	2.659(1)	2.688(1)	2.683(1)	2.652(1)
Ru(2)–Te(1)	2.586(1)	2.732(1)	2.688(1)	2.683(1)
Ru(3)–Te(1)	2.655(1)	2.710(1)	2.656(1)	2.636(1)
Ru(4)–Te(1)		2.696(1)		
Ru(1)–P(1)			2.333(1)	2.320(2) [b]
Ru(3)–P(2)			2.325(1)	2.336(2)
Ru(1)–H	1.85(5)		1.74(4) [a]	
Ru(3)–H	1.95(5)			
Ru(5)–H	1.95(5)			
Nb(1)–C(15)	2.057(5)	2.076(3)		
Nb(1)–C(16)	2.073(5)	2.073(3)		
Bond angles				
Ru(2)–Ru(1)–Ru(4)		88.2(1)		
Ru(2)–Ru(1)–Ru(6)	151.6(1)			
Ru(1)–Ru(2)–Ru(3)	66.7(1)		60.7(19	
Ru(1)–Ru(3)–Ru(5)	59.2(1)			
Ru(1)–Ru(5)–Ru(3)		89.3(1)		
Ru(1)–Te(1)–Ru(3)		97.9(1)	66.1(1)	97.9(1)
C(15)–Nb(1)–C(16)	86.3(2)	87.5(1)		

[a] Mean.
[b] Ru(2)–P(1).

temperature limit spectrum exhibits two RuH resonances at $\delta = -18.35$ and -17.57, what indicates hydride bridges in different environment. Concomittantly, at the same temperature there are two phosphorus resonances in the ^{31}P spectrum at $\delta = 21.3$ and 26.8.

The solid state structure of the molecule (Fig. 3) shows a Ru_3Te tetrahedron as the central feature with attached terminal CO ligands and the dppm ligand coordinated at Ru(1) and Ru(3). The difference Fourier synthesis reveals the presence of two hydride bridges, which are distributed throughout the Ru_3 triangle in an unsymmetrical manner. This finding is consistent with the low temperature NMR spectra. The bridged Ru–Ru bonds [average 2.942(1) Å] are significantly longer than the unbridged Ru(2)–Ru(3) bond [2.7898(5) Å] (Table 1).

Due to the difficulties in recognizing the true nature of **2** we employed in the beginning of our studies unconsciously mixtures of **2** and **5** for the reaction with dppm. From these reactions we got along with the above described tetrahedral cluster **6** another cluster which analyzed as $[Ru_3(CO)_7(dppm)Te_2]$ (**7**). In order to verify the source of this compound, we repeated the reaction of pure **5** with dppm, which has already been carried out by Mathur et al. [3]. Under similar reaction conditions (stoichiometry 1:1, CH_2Cl_2, 8 h, 20 °C), orange **7** and brown **8** were formed (Scheme 2). The latter turned out by means of analytical and spectroscopic data to be identical with the already published octahedral cluster $[Ru_4(CO)_9(dppm)(\mu_4\text{-}Te)_2]$ [3], whereas **7** was not observed in the previous reaction.

The composition of **7** was confirmed by means of FD mass spectrum and elemental analyses. The IR spectrum exhibits three strong absorptions typical of terminal CO groups, while the ^1H-NMR spectrum contain signals which may be assigned to the dppm ligand. The crystal structure determination of **7** reveals a Ru_3Te_2 square pyramid as the central feature (Fig. 4). The CO ligands are all terminally coordinated and the dppm ligand bridges the edge Ru(2)–Ru(3). The latter bond is longer by 0.075 Å than the unbridged Ru(1)–Ru(2) one. All Ru–Ru and Ru–Te distances are within the same range

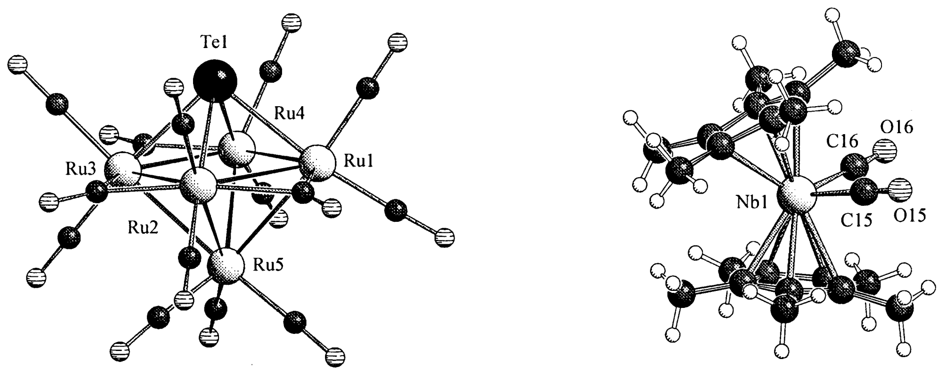

Fig. 2. Molecular structure of $[Ru_5H(CO)_{14}Te][Cp^*_2Nb(CO)_2]$ (**4**), anion left and cation right.

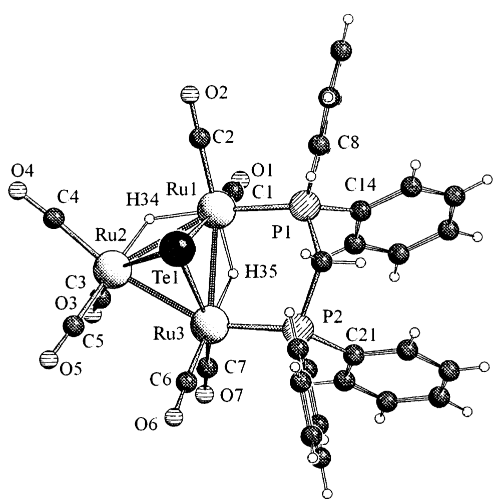

Fig. 3. Molecular structure of $[Ru_3H_2(CO)_7(dppm)Te]$ (**6**).

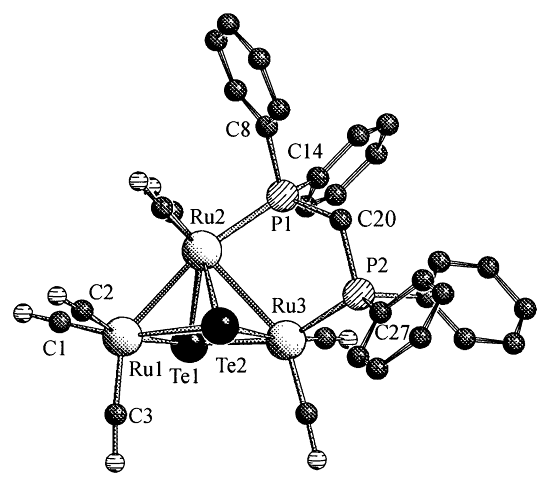

Fig. 4. Molecular structure of $[Ru_3(CO)_7(dppm)Te_2]$ (**7**).

observed for the other clusters reported in this paper and $[Ru_4(CO)_{11}(\mu_4\text{-}Te)_2]$ (**5**). The structure of **7** may be derived from that of **5** by removal of one $Ru(CO)_2$ vertex and subsequent substitution of two CO groups. Thus, **7** is like $[Ru_3(CO)_6(PPh_3)_3Te_2]$ [3] a further derivative of the class of 50 valence electron clusters $[M_3(CO)_9Te_2]$ (M = Fe [16], Os [17]) belonging to the nido-octahedral structure type.

2.3. Electrochemistry of 2 and 5

The electrochemical behavior of **2** has been studied by cyclic voltammetry and rotating disk electrode (RDE)

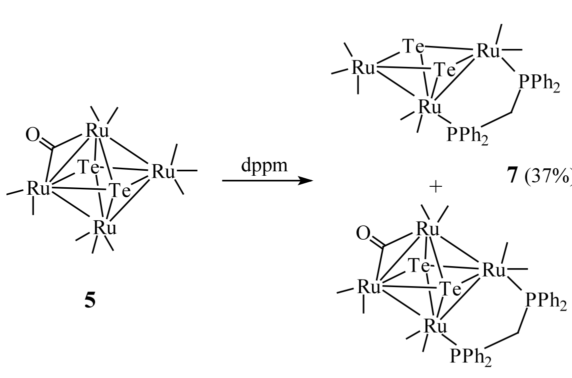

Scheme 2.

voltammetry. In the cathodic area, two irreversible systems have been obtained with $E_c = -1.26$ V and -2.18 V/SCE (saturated calomel electrode).

THF solutions of **5** exhibit in rotating disk electrode voltammetry three reduction steps at $E_{1/2} = -0.38$, -0.74 and -1.97 V/SCE. The height of these waves are in the ratio: 1:0.92:1.54. The second wave is smaller than the first one because the diffusing species may be $[Ru_4(CO)_{11}(\mu_4\text{-}Te)_2]^-$, which has a smaller diffusion coefficient than **5**.

In cyclic voltammetry three reversible systems are observed at sweep rates between 0.02 and 0.2 V s^{-1}. The two first waves are monoelectronic and the third one is bielectronic (Fig. 5). The ratio $i_p/v^{1/2}$ was verified to be constant and the ratio i_{pa}/i_{pc} was close to 1, in accord with diffusion control. The halfwave potentials are independent of potential scan rate and the peak shapes are characterized by $|E_{pc} - E_{pa}| \approx 60$ mV for the first two systems. The mechanism, at the time scale of cyclic voltammetry, is schematically given in Eq. (1).

$$\underset{\mathbf{5}}{[Ru_4(CO)_{11}Te_2]} \underset{A_1/A_2}{\overset{e^-}{\rightleftharpoons}} \underset{\mathbf{5}^-}{[Ru_4(CO)_{11}Te_2]^-} \underset{A_2/A_2'}{\overset{e^-}{\rightleftharpoons}} \underset{\mathbf{5}^{2-}}{[Ru_4(CO)_{11}Te_2]^{2-}} \underset{A_3/A_3'}{\overset{2e^-}{\rightleftharpoons}} \underset{\mathbf{5}^{4-}}{[Ru_4(CO)_{11}Te_2]^{4-}} \quad (1)$$

Some DFT/B3LYP/Lanl2DZ calculations [18] have been performed on **5** and on its reduced species **5**$^-$ and **5**$^{2-}$, respectively, showing that mainly the Ru(3)–Ru(4) distances are affected by reduction process. For the optimized structures these distances vary from 3.097 (neutral) through 3.222 (**5**$^-$) to 3.359 (**5**$^{2-}$) Å. Consequently, the dianion may exhibit a nido (pentagonal bipyramid) structure. Further reduction (e.g. **5**$^{3-}$) does not lead to convergence of metric parameters, what may indicate a rearrangement of the initial Ru_4Te_2 framework of **5**.

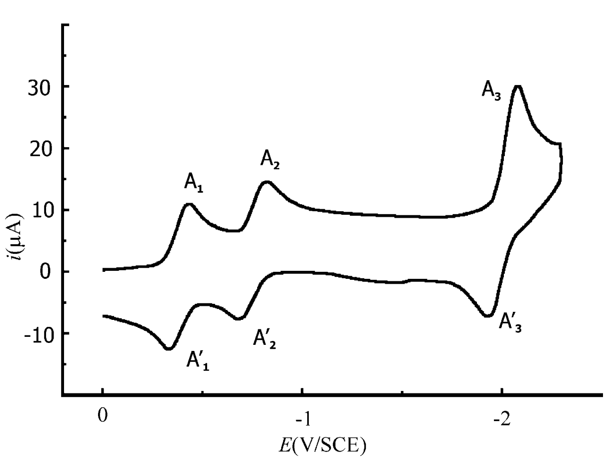

Fig. 5. Cyclic voltammogram of **5** in THF (0.2 mol l^{-1} of NBu_4PF_6) on a carbon electrode. Sweep rate: 0.1 V s^{-1}. Starting potential: 0 V.

This behavior may indicate an interesting ability of **5** for reversible and multiple electron uptake. In this regard **5** resembles homoleptic transition-metal carbonyl clusters with electron-sink features [19]. No other ruthenium chalcogenide cluster has been investigated before with respect to its redox properties. It may be noted that $[Ru_3(CO)_{12}]$ behaves completely different. The only reduction wave at -1.05 V is followed by rapid chemical reactions [20].

In conclusion, a new synthetic route for the formation of several neutral and salt-like ruthenium carbonyl clusters with telluride and hydride ligands has been found. It is striking that the compounds obtained are relatively poor in tellurium content giving rise to a preferential metal carbonyl character of the clusters and it has been impossible to increase the tellurium content by varying the stoichiometry of the title reaction. Further studies are necessary to explore the reactivity of the new compounds and to reveal whether the hydrogens in **3** and **4** arise from the Te_2H ligand in **1** or from the solvent.

3. Experimental

3.1. General and methods

All procedures were carried out under nitrogen using Schlenk techniques and dry solvents. Elemental analyses were performed by the Mikroanalytisches Laboratorium, Universität Regensburg. IR spectra were obtained with a Mattson Genesis Series FTIR instrument, ESI mass spectra and FD mass spectra were obtained on Finnigan TSQ 7000 and MAT 95 instruments, respectively. The ^{1}H-NMR and ^{31}P-NMR spectra were taken on a Bruker ARX 400 instrument at 400.1 and 161.9 MHz, respectively. $[Cp_2^*Nb(Te_2H)]$ (**1**) was prepared from $[Cp_2^*NbBH_4]$ and elemental tellurium [6]. Electrochemistry: cyclic voltammetry was carried out in a standard three-electrode cell with a Tacussel UAP4 unit cell. The reference electrode was a saturated calomel electrode (SCE) separated from the solution by a sintered glass disk. The auxiliary electrode was a platinum wire. For all voltammetric measurements, the working electrode was a vitreous carbon electrode. The

Table 2
Crystallographic data for complexes **3**, **4**, **6** and **7**

	3	**4**	**6**·CH_2Cl_2	**7**·C_7H_8
Formula	$C_{37}H_{31}NbO_{17}Ru_6Te_3$	$C_{36}H_{31}NbO_{16}Ru_5Te$	$C_{33}H_{26}Cl_2O_7P_2Ru_3Te$	$C_{39}H_{30}O_7P_2Ru_3Te_2$
Moleculat weight	1829.75	1444.46	1098.19	1230.98
Crystal size (mm)	0.28 × 0.20 × 0.18	0.30 × 0.16 × 0.04	0.60 × 0.42 × 0.24	0.24 × 0.12 × 0.06
Crystal system	Monoclinic	Triclinic	Triclinic	Triclinic
a (Å)	15.680(1)	11.418(1)	12.036(2)	9.949(1)
b (Å)	11.270(1)	13.872(2)	12.142(1)	20.224(2)
c (Å)	28.005(1)	15.119(1)	13.063(2)	22.378(2)
α (°)		75.39(1)	93.92(2)	104.42(1)
β (°)	91.81(1)	68.72(1)	93.23(2)	101.71(1)
γ (°)		88.49(1)	101.27(2)	100.11(1)
V (Å^3)	4946.3(5)	2153.6(4)	1863.0(3)	4146.8(6)
Space group	$P2_1/n$	$P\bar{1}$	$P\bar{1}$	$P\bar{1}$
Z	4	2	2	4
ρ_{calc} (g cm^{-3})	2.457	2.227	1.958	1.972
Instrument	Stoe IPDS	Stoe IPDS	Stoe IPDS	Stoe IPDS
Temperature (K)	173	173	173	173
μ (mm^{-1})	3.80	2.70	2.241	2.581
Absorption correction	numerical	numerical	numerical	numerical
Transmission	0.619/0.501	0.814/0.596	0.442/0327	0.895/0.705
Scan range	$1.95 < \Theta < 25.85.0$	$1.92 < \Theta < 25.82$	$2.69 < \Theta < 26.69$	$1.95 < \Theta < 25.84$
Total reflections	35081	30370	23893	34867
Observed reflections ($I > 2.0\sigma(I)$)	9372	7744	7293	11420
No. of LS parameters	580	532	439	955
Residual density (e Å^{-3})	0.704/−0.392	0.889/−0.366	1.063/−1.077	0.815/−0.511
R_1	0.022	0.018	0.026	0.027
wR_2	0.048	0.046	0.073	0.059

controlled potential electrolysis was performed with an Amel 552 potentiostat coupled to an Amel 721 electronic integrator. Electrolyses were performed in a cell with three compartments separated with fritted glasses of medium porosity. A carbon gauze was used as the cathode, a platinum plate as the anode and a saturated calomel electrode as the reference electrode.

3.2. Reaction of *1* with $[Ru_3(CO)_{12}]$

The mixture of 260 mg (0.42 mmol) of $[Cp^*_2Nb(Te_2H)]$ (**1**), 540 mg (0.84 mmol) of $[Ru_3(CO)_{12}]$ and 140 ml of toluene was refluxed for 18 h. After cooling the solvent was evaporated and the redbrown residue dissolved in 20 ml of CH_2Cl_2–toluene 3:1. Chromatography on SiO_2 (column 28 × 3 cm) gave upon elution with CH_2Cl_2–toluene 3:1 an orange–brown band and then two bands containing orange **3** (30 mg, 4% yield) and red–brown **4** (190 mg, 31%). Repeated chromatography of the first band gave after elution with pentane a yellow band containing **2** (65 mg, 11% yield) and an orange band. The latter has been identified by comparison of spectroscopic and analytical data as the known complex **5** (100 mg, 27%).

2: Anal. Found: C, 15.95; H, 0.41. Calc. for $C_9H_2O_9Ru_3Te$ (684.9): C, 15.78; H, 0.29%. FD MS 685. ^{1}H-NMR (CD_2Cl_2): δ −19.03 (s, 2H, RuH). IR (KBr, cm^{-1}): ν_{CO} 2112s, 2076s, 2041s, 2006s, 1978s.

3: Anal. Found: C, 24.32; H, 1.72. Calc. for $C_{37}H_{31}NbO_{17}Ru_6Te_3$ (1829.8): C, 24.28; H, 1.71%. NI-ESIMS (from CH_2Cl_2) 1410.4 ($[^{101}Ru_6H(CO)^{128}_{15}Te_3]^-$). ^{1}H-NMR ($CD_2Cl_2$): δ −36.45 (s, 1H, RuH), 1.94 (s, 30H, Me). IR (KBr, cm^{-1}): ν_{CO} 2066s, 2035s, 1993s, 1957s.

4: Anal. Found: C, 29.89; H, 2.29; Te, 8.01. Calc. for $C_{36}H_{31}NbO_{16}Ru_5Te$ (1445.5): C, 29.91; H, 2.16; Te, 8.86%. NI-ESIMS (from CH_2Cl_2) 1026.6 ($[^{101}Ru_5H(CO)^{128}_{14}Te]^-$). ^{1}H-NMR ($CD_2Cl_2$), δ −12.20 (s, 1H, RuH), 1.94 (s, 30H, Me). IR (CH_2Cl_2, cm^{-1}): ν_{CO} 2062s, 2010s, 1959s, 1814s.

3.3. Synthesis of $[Ru_3(\mu_2\text{-}H)_2(CO)_7(dppm)(\mu_3\text{-}Te)]$ (*6*)

The mixture of 120 mg (0.18 mmol) of **2**, 90 mg (0.23 mmol) of dppm and 100 ml of CH_2Cl_2 was stirred at room temperature (r.t.) for 10 h. After evaporation of the solvent the residue was dissolved in CH_2Cl_2–pentane 1:1 and chromatographed on SiO_2 (column 15 × 3 cm). Elution with CH_2Cl_2–pentane 1:1 gave a yellow–orange band containing 100 mg (56%) of **6**. The complex was recrystallized from CH_2Cl_2.

6: Anal. Found: C, 36.85; H, 2.52. Calc. for $C_{32}H_{24}O_7P_2Ru_3Te\cdot CH_2Cl_2$ (1098.2): C, 36.09; H, 2.39%. FDMS 1014.8 ($[^{101}Ru_3H_2(CO)_7(dppm)^{128}Te]^+$). $\{^{31}P\}^1$H-NMR (CD_2Cl_2, 183 K): δ −18.35 [d, 1H, RuH;

^2J(H–H) = 2.7 Hz], −17.57 [d, 1, RuH; ^2J(H–H) = 2.7 Hz], 3.69 [d, 1H, CH_2; ^2J(H–H) = 13.1 Hz], 3.87 [d, 1H, CH_2; ^2J(H–H) = 13.1 Hz], 7.10–7.54 (m, 20H, C_6H_5). $\{^1H\}^{31}P$-NMR (CD_2Cl_2, 183 K): δ 21.3 (^2J(P–P) = 53 Hz), 26.8 (^2J(P–P) = 53 Hz). IR (KBr, cm^{-1}): ν_{CO} 2057s, 2039s, 1999s, 1974s, 1944s.

3.4. Reaction of [$Ru_4(CO)_{11}Te_2$] (5) with dppm

The mixture of 100 mg (0.10 mmol) of **5**, 50 mg (0.13 mmol) of dppm and 70 ml of CH_2Cl_2 was stirred at r.t. for 8 h. After evaporation of the solvent the residue was purified by chromatography on SiO_2 (column 15 × 3 cm). Elution with CH_2Cl_2–pentane 2:1 gave an orange band containing 42 mg (36.8%) of **7**. A subsequent brown band contained 42 mg (32.4%) of **8**, which has been identified by comparison of IR and ^1H-NMR spectra with already known data [3].

7: Anal. Found: C, 37.64; H, 2.48. Calc. for $C_{32}H_{22}O_7P_2Ru_3Te_2 \cdot C_7H_8$ (1231.0): C, 38.05; H, 2.46%. FDMS 1140 ($[^{101}Ru_3(CO)_7(dppm)^{128}Te_2]^+$). ^1H-NMR (CD_2Cl_2): 4.19 [m, 2H, CH_2], 7.43–7.70 [m, 20H, C_6H_5]. IR (KBr, cm^{-1}): ν_{CO} 2057s, 1996vs, 1944s.

3.5. X-ray structure solution

The structures of **3**, **4**, **6** and **7** were solved by direct methods and refined by full-matrix least-squares techniques with the program SHELXL-97. Subsequent difference Fourier syntheses revealed the position of the non-hydrogen atoms and all these atoms were refined with anisotropic thermal parameters. All H atoms attached to C were calculated geometrically and a riding model was used during refinement process. The hydrogen bridges in the structures of **3** [H(1)] and **6** [H(34, 35)] were found in the difference Fourier map. Details for the structure refinements are listed in Table 2.

4. Supplementary material

Crystallographic data for the structural analysis have been deposited with the Cambridge Crystallographic Data Centre, CCDC nos. 171078 (**3**), 171079 (**4**), 182718 (**6**) and 182719 (**7**), respectively. Copies of this information may be obtained free of charge from The Director, CCDC, 12 Union Road, Cambridge CB2 1EZ, UK (Fax: +44-1223-336033; e-mail: deposit@ccdc.cam.ac.uk or www: http://www.ccdc.cam.ac.uk).

Acknowledgements

We are grateful to the Deutsche Forschungsgemeinschaft for financial support. Parts of this work were supported by the Deutscher Akademischer Auslandsdienst and the Ministère des Affaires Etrangères (program PROCOPE).

References

[1] A.J. Deeming, in: E.W. Abel, F.G.A. Stone, G. Wilkinson (Eds.), Comprehensive Organometallic Chemistry, vol. 7, Pergamon, Oxford, 1995, p. 726.
[2] D. Cauzzi, C. Graiff, G. Predieri, A. Tiripicchio, in: P. Braunstein, L.A. Oro, P.R. Raithby (Eds.), Metal Clusters in Chemistry, vol. 1, Wiley-VCH, New York, 1999, p. 193.
[3] P. Mathur, B.H.S. Thimmappa, A.L. Rheingold, Inorg. Chem. 23 (1990) 4658.
[4] S.-P. Huang, M.G. Kanatzidis, J. Am. Chem. Soc. 114 (1992) 5477.
[5] (a) J.W. Kolis, Coord. Chem. Rev. 105 (1990) 195;
(b) L.C. Roof, J.W. Kolis, Chem. Rev. 93 (1993) 1037.
[6] O. Blacque, H. Brunner, M.M. Kubicki, B. Nuber, B. Stubenhofer, J. Wachter, B. Wrackmeyer, Angew. Chem. Int. Ed. Engl. 36 (1997) 351.
[7] (a) H. Brunner, D. Lucas, T. Monzon, Y. Mugnier, B. Nuber, B. Stubenhofer, A.C. Stückl, J. Wachter, R. Wanninger, M. Zabel, Chem. Eur. J. 6 (2000) 493;
(b) H. Brunner, A.C. Stückl, J. Wachter, R. Wanninger, M. Zabel, Angew. Chem. Int. Ed. Engl. 40 (2001) 2529.
[8] E. Sappa, O. Gambino, G. Cetini, J. Organomet. Chem. 35 (1972) 375.
[9] B.F.G. Johnson, J. Lewis, P.G. Lodge, P.R. Raithby, J. Chem. Soc. Chem. Commun. (1979) 719.
[10] L.C. Roof, D.M. Smith, G.W. Drake, W.T. Pennington, J.W. Kolis, Inorg. Chem. 34 (1995) 337.
[11] H.T. Schacht, A.K. Powell, H. Vahrenkamp, M. Koite, H.J. Kneuper, J.R. Shapley, J. Organomet. Chem. 368 (1989) 269.
[12] U. Bodensieck, H. Stoeckli-Evans, G. Süss-Fink, Angew. Chem. Int. Ed. Engl. 30 (1991) 1126.
[13] H. Brunner, J. Wachter, R. Wanninger, M. Zabel, J. Organomet. Chem. 603 (2000) 135.
[14] C.J. Gilmore, P. Woodward, J. Chem. Soc. A (1971) 3453.
[15] R.D. Adams, J.E. Babin, M. Tasi, Organometallics 7 (1988) 503.
[16] (a) W. Hieber, J. Gruber, Z. Anorg. Allg. Chem. 296 (1958) 91;
(b) D.A. Lesch, T.B. Rauchfuss, Inorg. Chem. 20 (1981) 3583;
(c) D.A. Lesch, T.B. Rauchfuss, Organometallics 1 (1982) 499;
(d) H. Schumann, M. Magerstädt, J. Pickardt, J. Organomet. Chem. 240 (1982) 407.
[17] J. Zhang, W.K. Leong, J. Chem. Soc. Dalton Trans. (2000) 1249.
[18] E. Vigier, M.M. Kubicki, Private communication.
[19] G. Longoni, C. Femoni, M.C. Iapalucci, P. Zanello, in: P. Braunstein, L.A. Oro, P.R. Raithby (Eds.), Metal Clusters in Chemistry, vol. 2, Wiley-VCH, New York, 1999, p. 1137.
[20] (a) A.J. Downard, B.H. Simpson, A.M. Bond, J. Organomet. Chem. 320 (1987) 363;
(b) M.I. Bruce, J.G. Matisons, B.K. Nicholson, J. Organomet. Chem. 247 (1983) 321.